Int. J. Electrochem. Sci., 7 **(2012)** 7567 - 7578

International Journal of ELECTROCHEMICAL SCIENCE
www.electrochemsci.org

Effects of Grain Refinement on the Corrosion Behaviour of Microalloyed Steel in Sulphuric Acid Solutions

El-Sayed M. Sherif [1,2] *and Asiful H. Seikh* [1,*]

[1] Center of Excellence for Research in Engineering Materials (CEREM), College of Engineering, King Saud University, P. O. Box 800, Al-Riyadh 11421, Saudi Arabia
[2] Electrochemistry and Corrosion Laboratory, Department of Physical Chemistry, National Research Centre (NRC), Dokki, 12622 Cairo, Egypt
[*]E-mail: aseikh@ksu.edu.sa

Received: 16 May 2012 / *Accepted:* 6 July 2012 / *Published:* 1 August 2012

Microalloyed steels have been widely used in many applications, particularly in car bodies and other engineering parts. This is because these steels are characterized by their high strength and high ductility. The combination of strength and ductility for these steels are usually resulting from the very fine grained microstructure. In the current work, the effects of grain refinement on the corrosion resistance property of BSK 46 microalloyed steel in 1N H_2SO_4 solution under different microstructural conditions were reported. The repeated quenching of the BSK 46 steels was found to increase the refining in their microstructures. Effects of changing temperature on the corrosion properties of the steel were also investigated at three different temperatures namely, 20 ^{0}C, 30 ^{0}C and 40 ^{0}C. The corrosion behaviour of the steel was investigated using galvanostatic polarization. It was found that repeating the quenching of steel, grains become finer and corrosion rate increases suggesting that a compromise has to strike between high mechanical property and corrosion rate.

Keywords: corrosion behaviour; galvanostatic polarization; microalloyed steels; sulphuric acid; quenching

1. INTRODUCTION

Microalloyed Steel has a ferritic matrix that of a mild steel but with an extremely fine grained structure. Alloying additions of niobium and titanium of the order of micro additions brings this refinement in the microstructure. The combination of high strength and ductility of this steel is due to the very fine grain structure. Without change in other microconstitutional properties the grain refinement of ferritic microalloyed steels is done by repeated quenching from a temperature just below the lower critical temperature i.e. in the ferritic region as reported in literature [1,2]. The effects of microstructure on the corrosion behaviour of steel are still an open field for investigation to correlate the metallurgical concept with the corrosion parameters. Only few authors [3-7] have investigated the influence of heat treatment on corrosion behavior of steel in different solutions.

We have been studying corrosion and corrosion inhibition of iron [8-11], copper [12-29], Monel-400 [30-32], aluminum [33-40], magnesium [41-44] and duplex stainless steels [45-49] in a variety of media. In our previous studies [8-11], the corrosion and corrosion inhibition of iron in aerated 3.5% NaCl solutions by 3-amino-5-mercapto-1,2,4-triazole, 5-(3-aminophenyl)-tetrazole, and 1,1'-thiocarbonyldiimidazole using in situ and ex situ Raman spectroscopy, cyclic voltammetry, open-circuit potential, potentiodynamic polarization, potentiostatic current-time and electrochemical impedance spectroscopy have been reported. The effects of exposure time and elemental additives as well as corrosion inhibitors on the mechanism of corrosion and corrosion inhibition of Monel-400, magnesium, aluminum, copper and stainless steel [30-49] neutral and acidic solutions have been also investigated.

In the present study, corrosion property of as rolled and repeatedly quenched microalloyed steels in sulphuric acid solution has been studied by galvanostatic polarization techniques at three different temperatures, namely 20 ^{0}C, 30 ^{0}C and 40 ^{0}C. One of the most important fields of application for the steel in sulphuric acid is in acid pickling, industrial acid cleaning, acid descaling and oil well acidizing. It is well known that the material that are used in heating and cooling systems such as steels suffer from scale and corrosion products formation. Scale and corrosion products have a negative effect on both heat and solution transfer, which causes a decrease in heating efficiencies of the equipment and the quantity and velocity of the solution. This is why periodic de-scaling and cleaning in sulphuric acid pickling solutions are necessary.

2. EXPERIMENTAL DETAILS

2.1. Materials

The material, which is commonly called Nb-bearing commercial microalloyed steel BSK 46 grade with chemical composition as fellows: 0.12 wt. %C, 1.0 wt. %Mn, 0.025 wt. % S, 0.025 wt. % P, 0.10 wt. % Si, 0.02-0.07 wt. % Al, and 0.08 wt. % Nb with the balance is Fe.

2.2. Heat Treatment

All heat treatment cycles were carried out in a Muffle Furnace coupled with a proportional temperature controller with an accuracy level of ± 20 ^{0}C. The furnace atmosphere was not controlled.

2.3. Sample Preparation

One of the surfaces of the each metallographic specimens as received [designates as AR], first quench (Q1), second quench (Q2), and third quench (Q3) of each grade were grounded mechanically on the silicon carbide abrasive papers sequentially on 60, 120, 240, 320, 400, 600 grit silicon carbide papers and polished on a Selvyt cloth using coarse and fine Geosyn- Grade I slurry of Al_2O_3. Specimens were cleaned, washed by water and then by alcohol and dried. All the polished specimens were etched using 2.0 % Nital (2.0 % HNO_3 in Methanol) solution. With these polished and etched samples optical microscopy, grain size measurement and hardness testing were carried out.

2.4. Optical microscopy, grain size measurement and hardness testing

The etched specimens were tested one by one using an optical microscope. The photographs of the microstructure were taken with help of a Camera fitted with a microscope.

The grain size of each specimen was measured by using a real image analysis with the help of an image analyzing software, Biovis Material Plus- version 1.3.

Vickers hardness of the metallographic specimens were carried out in a standard Vickers hardness testing machine using square-base diamond pyramid as the indenter and a load of 30kg as per ASTM Standard E92-72. Tests were carried out at least in three different positions on the polished surface of the specimens and the average Vickers hardness value was reported.

2.5. Corrosion tests

The test solution was 1N H_2SO_4 prepared from the laboratory grade of H_2SO_4 and distilled water. Electrochemical experiments were performed in a conventional three-electrode electrochemical cell containing 600ml solution. The microalloy steel strips were the working electrode (WE), graphite rod was the counter electrode and saturated calomel electrode (SCE) was the reference electrode.

Steel specimens were machined into a cubical form with an exposed area 1 cm^2. An insulated copper wire was secured to one of the surface of each steel specimen with solder at low temperature. The specimens were mounted with epoxy resin in such a way that only the other flat surface contacted with the solution. This flat surface of each specimen was polished mechanically in graded emery paper and final finish was given on a polishing wheel using alumina powder. The polished surface was then thoroughly washed and digressed in ethanol before used and dried at room temperature.

Anodic and cathodic corrosion potentials were recorded in Volts vs. SCE for various current values of current densities at three different temperature viz. 20^0C, 30^0C and 40^0C. For each individual run the surface of the specimen was ground and polished freshly, washed and digressed in ethanol and dried in warm air.

3. RESULTS AND DISCUSSION

3.1. Metallographic studies of the microalloyed steel

Figure 1 shows the microstructure of (a) as received, (b) first quench, (c) second quench, and (d) third quenched BSK 46 (the magnifications for all specimens were 4x40 X). The variation of the grain size number with the change of the quenching temperature is also listed in Table 1. It is clearly seen from Fig. 1 that the grain size is bigger for the as received sample and gets finer with quenching and further with repeating the number of quenching up to the third time. The numerical values of the grain size recorded in Table 1 in addition to the images shown in Fig. 1 confirm that the ferritic grain size decreases with repeating the quench from first to third quench. Here, the ASTM grain size number of the as received sample was reported to be 9.1, increased due to first quenching to 9.7, and further increased to 10.5 for second quenching and finally recorded the highest value, 10.8, with repeating the process to the third quenching. This is because the repeated quenching leads to repeated recrystallization, which in turn leads to producing new grains at the expense of others and a coarse grained material (as rolled) replaces the fine grained recrystallized structure. This concludes that increasing the repeated quenching increases the ASTM grain size number and therefore decreases the grain size.

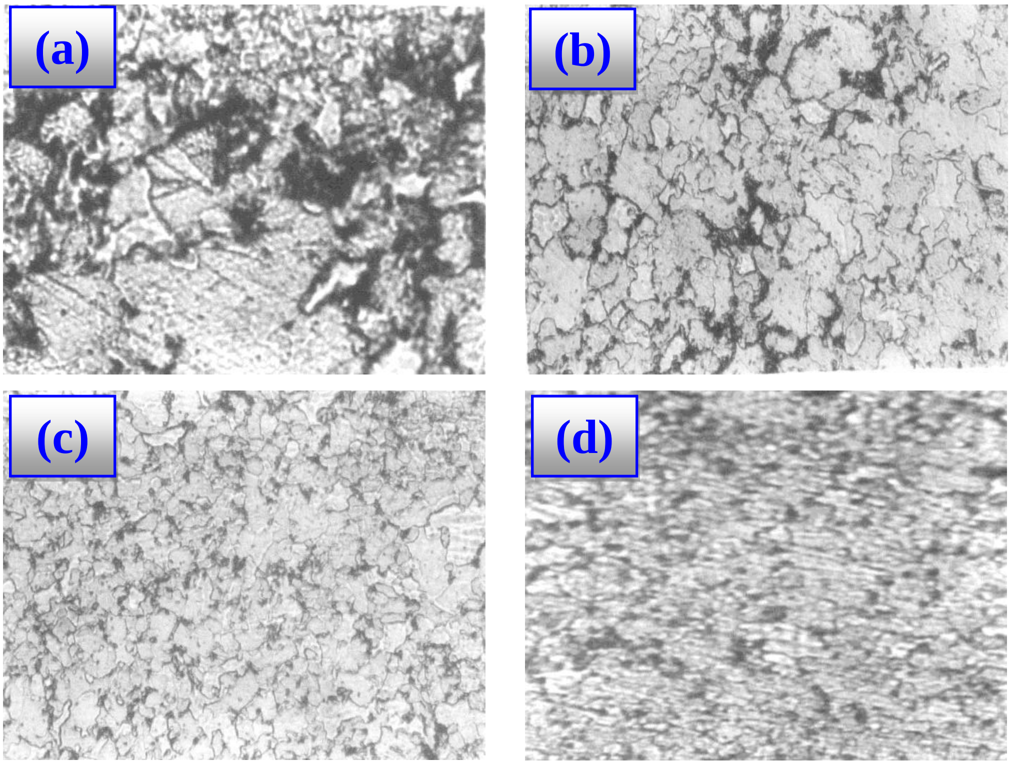

Figure 1. The microstructure of (a) as received, (b) first quench, (c) second quench, and (d) third quenched microalloyed BSK 46 steel; all magnifications were 4x40 X.

The variation of the Vickers hardness number (VHN) for the test specimens with the number of the repeated quenching is listed in Table 2. It is shown from Table 2 that the hardness values for the as received BSK 46 sample recorded 195 VHN. This value increased to 201 VHN, 210 VHN and 215 VHN when the repeated quenching for the tested specimen was increased from first quench to second quench and further to third quench sample, respectively. This increase in the hardness values with increasing the repeated quenching is attributed to the grain refinement of the ferritic microalloyed BSK 46 steel.

Table 1. ASTM grain size number for the tested specimens

As Received	First Quench	Second Quench	Third Quench
9.1	9.7	10.5	10.8

Table 2. Vickers hardness number (VHN) for the test specimens

As Received	First Quench	Second Quench	Third Quench
195	201	210	215

3.2. Effect of temperature and grain refinement on corrosion behaviour

The linear polarization behaviour for the as received microalloy BSK 46 steel at 20 ^{o}C in 1N H_2SO_4 solution was recorded in a potential range between -0.76 and -0.55 V vs. SCE and the curve is shown in Fig. 2. It is clear from Fig. 2 that the best straight line through the linear polarization points was drawn and the values of anodic, β_a, and cathodic, β_c, (values are not listed) were calculated from the straight line in the anodic and cathodic branches, respectively [23-28]. As will as, the values of corrosion current (j_{Corr}) and corrosion potential (E_{Corr}) for the as received BSK 46 steel were obtained from the extrapolation of anodic and cathodic Tafel lines located next to the linearized current regions and according to our previous studies [30-37]. It was found that the values of β_a and β_c were close to each other but with different sign i.e. β_a was positive and β_c was negative.

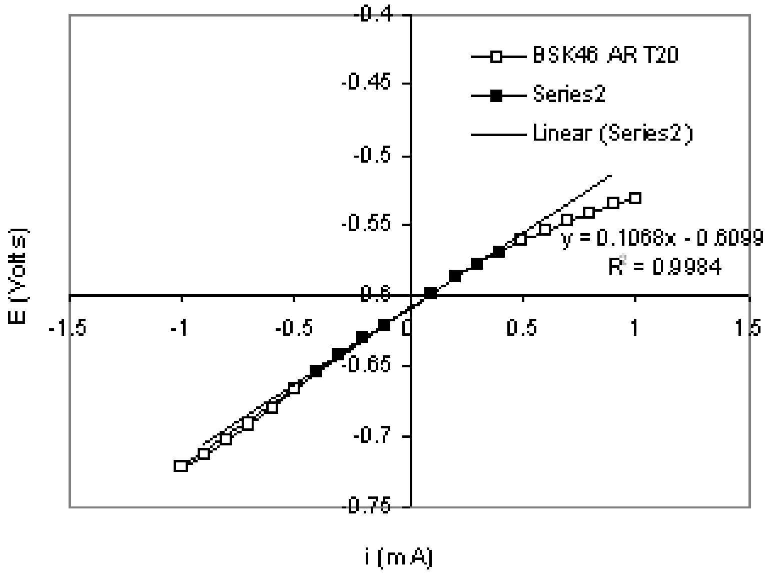

Figure 2. Linear polarization behaviour of the as received microalloyed BSK 46 steel in 1N H_2SO_4 solution at 20 ^{0}C.

The galvanostatic anodic and cathodic polarization curves for the as received microalloyed BSK 46 steel in 1N H_2SO_4 solution at 20 ^{0}C were carried out as shown in Fig. 3. The values of E_{Corr} and j_{Corr} were calculated and listed in Table 3. The cathodic reaction for steel in acidic solution has been reported to be the evolution of hydrogen as the electron consumption on steel happens by the unloading of hydrogen ions as follows [42],

$$2H^+ + 2e^- = H_2 \qquad (1)$$

Here, the source of the hydrogen ions (more exactly the hydronium ion H_3O) is the dissociated water, according to the following reaction;

$$H_2O = H^+ + OH^- \qquad (2)$$

On the other hand, the anodic reaction of steel at the same condition is the dissolution of iron as fellows,

$$Fe = Fe^{2+} + 2e^- \qquad (3)$$

The electrons produced by the anodic reactions are consumed at the cathode. It has been reported [50] that the formation of iron oxide, FeO, in the presence of water can be formed in sulphuric acid solution at less negative potential than E_{Corr} and in the anodic branch according to the following reaction;

$$Fe + H_2O = FeO + 2H^+ + 2e^- \qquad (4)$$

The formation of higher iron oxide, Fe_2O_3 was also reported [50] to occur at much less negative potential of steel in the acid solution,

$$2FeO + H_2O = Fe_2O_3 + 2H^+ + 2e^- \qquad (5)$$

It is seen from Fig. 3 that irons dissolves rapidly in the test solution as the current rapidly increases with increasing the applied potential. The oxides formed via reactions shown in Eq. 4 and Eq. 5 were not stable and not protective enough to enable iron to resist the severity of the sulphuric acid solution. This is also because sulphuric acid attacks the iron surface in a way that does not allow any corrosion products or oxide films to be developed and if formed not thickened and thus no protection is provided for iron surface against corrosion. This agrees with the work reported by Wang and Kido [51] that the corrosion occurred on the surface of iron in sulphuric acid is mostly general with small corrosion dents appear on the surface by locally preferable corrosion.

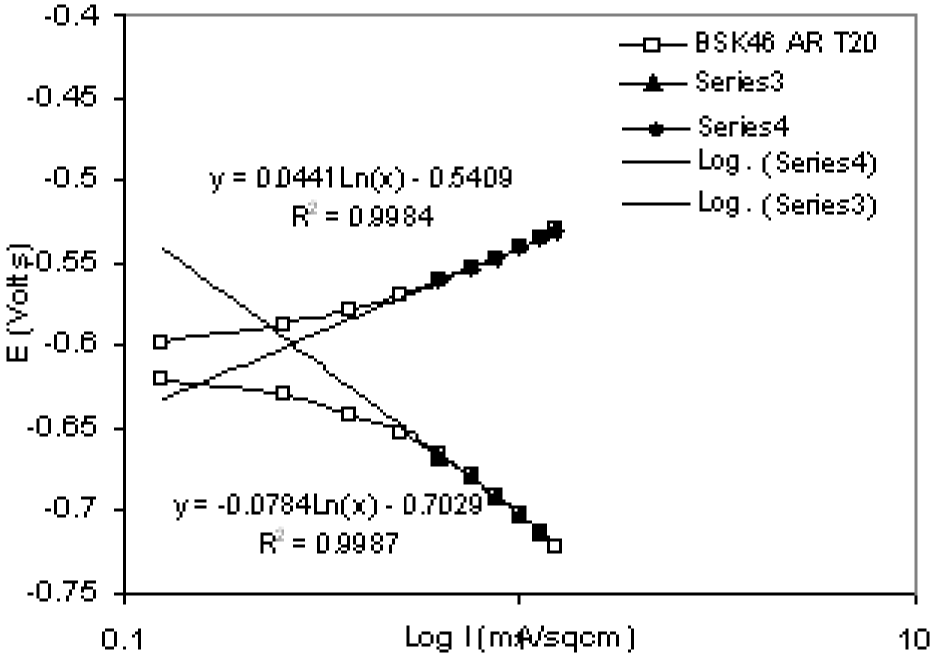

Figure 3. Galvanostatic polarization behaviour of as received BSK 46 steel in 1N H_2SO_4 at 20^0 C.

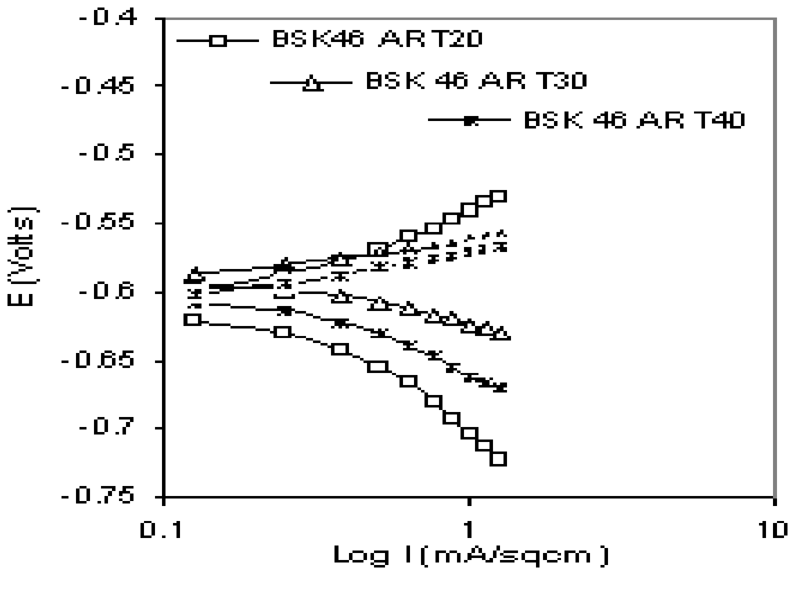

Figure 4. Galvanostatic polarization of as received microalloyed BSK 46 steel in 1N H_2SO_4 at 20 ^oC, 30 ^oC, and 40 ^oC.

In order to study the effect of temperature on the dissolution of the as received microalloy BSK 46 steel in 1N H_2SO_4, the galvanostatic polarization measurements were performed for steel at 20^0C, 30^0C, and 40^0C and the curves are shown in Fig. 4. The values of E_{Corr} and j_{Corr} obtained from the polarization curves shown in Fig. 4 are listed in Table 3. It is seen from Fig. 4 and Table 3 that increasing the temperature from 20^0C to 30^0C increase the rate anodic and cathodic reactions, which increases the values of j_{Corr} from 0.275mA/cm^2 to 0.285mA/cm^2; this effect highly increased the values of j_{Corr}, 0.35mA/cm^2, when the temperature was increased to 40^{0}C. This indicates that the increase of solution temperature activates the corrosion of BSK 46 microalloyed steel through increasing both cathodic (Eq. 1) and anodic (Eq. 3) reactions, shifting the corrosion potential slightly towards the less negative values and increasing the corrosion currents and thus the corrosion rates.

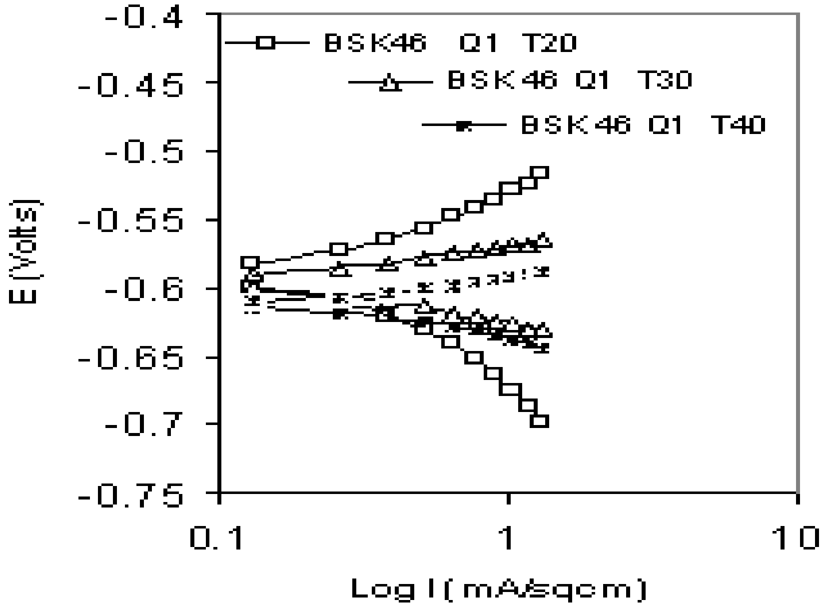

Figure 5. Galvanostatic polarization behaviour after the first quench of the microalloyed BSK 46 steel in 1N H_2SO_4 at 20 ^oC, 30 ^oC, and 40 ^oC, respectively.

The effects of both grain size and temperature on the corrosion current density of BSK 46 microalloyed steels in different microstructural viz. as rolled condition and three repeated quenched conditions in 1N H_2SO_4 solution were studied. This was to see whether the repeated quench with changing solution temperature would increase or decrease the corrosion process for the BSK 46 microalloyed steel in the sulphuric acid solution using the galvanostatic polarization measurements. Fig. 5 shows the galvanostatic polarization curves obtained for the first quenched BSK 46 microalloyed steel after 20 ^oC, 30 ^oC, and 40 ^oC, respectively. The corrosion parameters obtained from Fig. 5 is recorded in Table 3. It is obvious from Fig. 4, Fig. 5 and Table 3 that the corrosion reactions of steel increased by its quenching at all the tested temperatures. Quenching the steel increased its corrosion currents from 0.275, 0.285 and 0.35 mA/cm^2 to 0.31, 0.33 and 0.37mA/cm^2 at 20 ^oC, 30 ^oC, and 40 ^oC, respectively. It is also seen that increasing the temperature for the quenched steel increased the corrosion currents and thus increased the corrosion current due to increasing the steel anodic and cathodic reactions. Unlike the as received steel, the corrosion potential was negatively shifted with increasing the temperature, where the value of E_{Corr} recorded -0.590 V at 20 ^oC, shifted to -0.596 V at 30 ^oC, and further to -0.613 V at 40 ^oC. This indicates that both quenching and temperature increase the corrosion of BSK 46 steel in 1N H_2SO_4 solution.

Table 3. The values of corrosion potential (E_{Corr}, V vs. SCE) and corrosion current (j_{Corr}, mA/cm^2) of BSK 46 steel before and after 1st, 2nd and 3rd quench in 1N H_2SO_4 solutions.

Temp.	Treatment							
	As received		First quench		Second quench		Third quench	
	E_{Corr}	j_{Corr}	E_{Corr}	j_{Corr}	E_{Corr}	j_{Corr}	E_{Corr}	j_{Corr}
20 °C	-0.608	0.275	-0.590	0.31	-0.585	0.34	-0.598	0.35
30 °C	-0.589	0.285	-0.596	0.33	-0.606	0.41	-0.605	0.41
40 °C	-0.603	0.35	-0.613	0.37	-0.583	0.42	-0.592	0.43

The galvanostatic polarization anodic and cathodic curves after the second quench for the BSK 46 microalloyed steel in 1N H_2SO_4 solution at 20 °C, 30 °C, and 40 °C are shown in Fig. 6. The same curves for BSK 46 microalloyed steel in 1N H_2SO_4 solution at the same temperatures are also represented in Fig. 7. The values for corrosion potential and current are also reported in Table 3. Repeating the quench for the second time, Fig. 6, led to an increase in the value of the measured corrosion current compared to the as received steel and further to the first quenched sample. The increase of the H_2SO_4 solution temperature after the second quench for the steel was also found to greatly increase the corrosion current; these j_{Corr} values were higher than those recorded for the as received and first quenched steel.

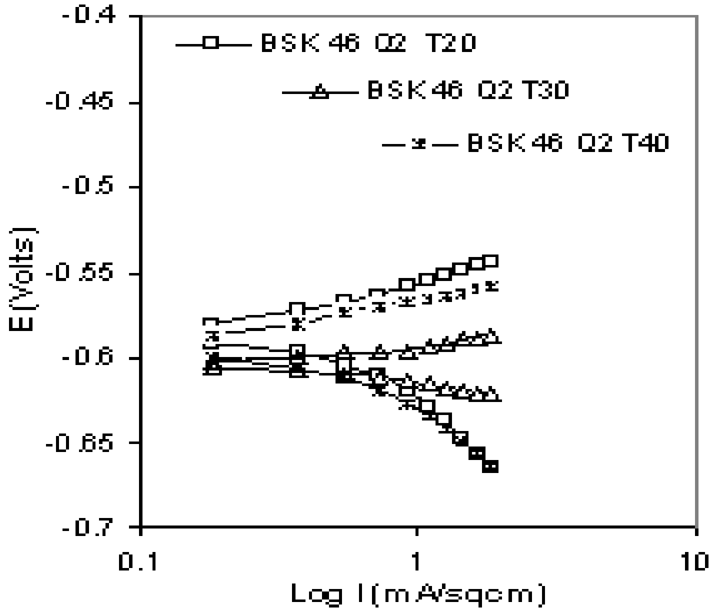

Figure 6. Galvanostatic polarization of the second quench of the microalloyed BSK 46 in 1N H_2SO_4 at 20 °C, 30 °C, and 40 °C.

It is seen from Fig. 7 and Table 3 that the highest corrosion current was recorded for the steel in the test solution was after the third quench. This effect is highly increased with increasing the temperature of the H_2SO_4 solution from 20 °C to 40 °C. This means that the achieved grain refinement in repeated quenching up to the third greatly rendered the anodic area than coarser grained structure, which led to the increase of the corrosion current values and hence the corrosion rate. It is worth to mention that there was no definite variation in the corrosion potential, E_{Corr}, took place for the as received and the increase of the quenching time number.

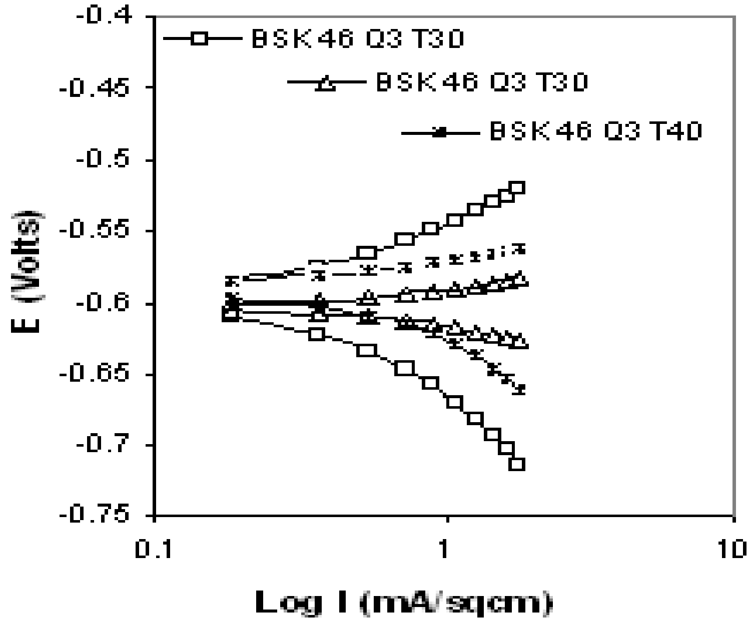

Figure 7. Galvanostatic polarization of the third quench of the microalloyed BSK 46 in 1N H_2SO_4 at 20 °C, 30 °C, and 40 °C.

4. CONCLUSION

The effects of grain refinement on the corrosion of BSK 46 microalloyed steel in 1N H_2SO_4 solutions after different microstructural conditions and temperatures have been investigated. Due to repeated quenching from a temperature just below the lower critical temperature the grain refinement of ferritic microalloyed steel has been achieved. Repeating the quenching up to three times led to yielding new grains at the expense of others and a coarse grained material (as rolled) is replaced by the fine grained recrystallized structure. Increasing the temperature of the sulphuric acid solutions from 20 °C to 40 °C both for as received and quenched steel enhanced its corrosion current values and accelerated its dissolution rate. The same effect was achieved by quenching the steel and repeating the quenching number up to three times. The repeated quenching refines the grains, which renders greater anodic areas than coarser grained structure and thus activates the corrosion of steel. It was also found that the increase of the temperature of the solution as well as the quenching time number don't have a pronounced variation in the values of the corrosion potential of the BSK 46 microalloyed steel.

ACKNOWLEDGEMENTS

The author extends his appreciation to the Deanship of Scientific Research at KSU for funding the work through the research group project No. RGP-VPP-160.

References

1. S. Sen, R. Priestner, *Trans. Indian Inst. Met.*, 37 (1984) 485.
2. R.A. Grange, Refinement of austenite grains due to successive recrystallization, *Trans. ASM*, 59 (1966) 26.
3. H.H. Uhlig, *Corrosion and Corrosion Control*, Wiley, New York (1963) P. 109-111.
4. H. Luo, Y.C. Guan, K.N. Han, *Corrosion*, 54 (1998) 619-627.
5. M.E. Kamp, H.E. Trout, *Corrosion*, 24 (1968) 11.
6. H.J. Cleary, N.D. Greene, *Corros. Sci*., 7 (1969) 821.
7. H.J. Cleary, N.D. Greene, *Corros. Sci*., 9 (1969) 3.
8. El-Sayed M. Sherif, R.M. Erasmus, J.D. Comins, *Electrochim. Acta,* 55 (2010) 3657.
9. El-Sayed M. Sherif, *Int. J. Electrochem. Sci.*, 6 (2011) 3077.
10. El-Sayed M. Sherif, *Mater. Chem. Phys*., 129 (2011) 961.
11. El-Sayed M. Sherif, Corrosion Inhibition in Chloride Solutions of Iron by 3-Amino-1,2,4-triazole-5-thiol and 1,1'-Thiocarbonyldiimidazole, *Int. J. Electrochem. Sci.*, 7 (2012) In Press.
12. El-Sayed M. Sherif, *Int. J. Electrochem. Sci.*, 7 (2012) 1482.
13. El-Sayed M. Sherif, *Int. J. Electrochem. Sci.*, 7 (2012) 1884.
14. El-Sayed M. Sherif, *Int. J. Electrochem. Sci.*, 7 (2012) 2832.
15. El-Sayed M. Sherif, R.M. Erasmus, J.D. Comins, *J. Appl. Electrochem*., 39 (2009) 83.
16. El-Sayed M. Sherif, *J. Appl. Surf. Sci*., 252 (2006) 8615.
17. E.M. Sherif, S.-M. Park, *J. Electrochem. Soc*., 152 (2005) B205.
18. El-Sayed M. Sherif, R.M. Erasmus, J.D. *Comins, Corros. Sci.*, 50 (2008) 3439.
19. A. El Warraky, H.A. El Shayeb, E.M. Sherif, *Anti-Corros. Method. Mater.*, 51 (2004) 52.
20. El-Sayed M. Sherif, R.M. Erasmus, J.D. Comins, *J. Colloid Interface Sci*., 306 (2007) 96.
21. El-Sayed M. Sherif, R.M. Erasmus, J.D. Comins, *J. Colloid Interface Sci*., 309 (2007) 470.
22. El-Sayed M. Sherif, R.M. Erasmus, J.D. Comins, *J. Colloid Interface Sci*., 311 (2007) 144.
23. El-Sayed M. Sherif, A.M. El Shamy, M.M. Ramla, A.O.H. El Nazhawy, *Mater. Chem. Phys*., 102 (20007) 231.
24. El-Sayed M. Sherif, *J. Mater. Eng. Performance,* 19 (2010) 873.
25. El-Sayed M. Sherif, A.H. Ahmed, *Synthesis and Reactivity in Inorganic, Metal-Organic, and Nano-Metal Chemistry*, 40 (2010) 365.
26. E. M. Sherif, S.-M. Park, *Corros. Sci.*, 48 (2006) 4065.
27. E.M. Sherif, S.-M. Park, Electrochim. Acta 51 (2006) 4665.
28. E.M. Sherif, S.-M. Park, *Electrochim. Acta*, 51 (2006) 6556.
29. El-Sayed M. Sherif, A.A. Almajid, *J. Appl. Electrochem.*, 40 (2010) 1555.
30. El-Sayed M. Sherif, *J. Solid State Electrochem.*, 16 (2012) 891.
31. El-Sayed M. Sherif, A.A. Almajid, A.K. Bairamov, Eissa Al-Zahrani, *Int. J. Electrochem. Sci.*, 6 (2011) 5430.
32. El-Sayed M. Sherif, A.A. Almajid, A.K. Bairamov, Eissa Al-Zahrani, *Int. J. Electrochem. Sci.*, 7 (2012) 2796.
33. E.M. Sherif, S.-M. Park, *J. Electrochem. Soc*., 152 (2005) B428.
34. E.M. Sherif, S.-M. Park, *Electrochim. Acta*, 51 (2006) 1313.
35. El-Sayed M. Sherif, E.A. El-Danaf, M.S. Soliman, A.A. Almajid, *Int. J. Electrochem. Sci.*, 7 (2012) 2846.
36. F.H. Latief, El-Sayed M. Sherif, A.A. Almajid, H. Junaedi, *J. Anal. Appl. Pyrolysis,* 92 (2011) 485.
37. El-Sayed M. Sherif, A.A. Almajid, F.H. Latif, H. Junaedi, *Int. J. Electrochem. Sci.*, 6 (2011) 1085.
38. El-Sayed M. Sherif, F.H. Latif, H. Junaedi, A.A. Almajid, *Int. J. Electrochem. Sci.*, 7 (2012) 4352.
39. El-Sayed M. Sherif, *Int. J. Electrochem. Sci.*, 6 (2011) 1479.

40. El-Sayed M. Sherif, Effects of 3-Amino-1,2,4-triazole-5-thiol on the Inhibition of Pure Aluminum Corrosion in Aerated Stagnant 3.5 wt.% NaCl Solution as a Corrosion Inhibitor, *Int. J. Electrochem. Sci.*, 7 (2012) In Press.
41. El-Sayed M. Sherif, *Int. J. Electrochem. Sci.*, 7 (2012) 4235.
42. El-Sayed M. Sherif, A.A. Almajid, *Int. J. Electrochem. Sci.*, 6 (2011) 2131.
43. Khalil A. Khalil, El-Sayed M. Sherif, A.A. Almajid, *Int. J. Electrochem. Sci.*, 6 (2011) 6184.
44. El-Sayed M. Sherif, A Comparative Study on the Effects of 5-(3-Aminophenyl)-tetrazole on the Inhibition of Magnesium Corrosion in Natural Seawater and 3.5% NaCl Solutions, *Int. J. Electrochem. Sci.*, 7 (2012) In Press.
45. J.H. Potgieter, P.A. Olubambi, L. Cornish, C.N. Machio, El-Sayed M. Sherif, *Corros. Sci*., 50 (2008) 2572.
46. El-Sayed M. Sherif, J.H. Potgieter, J.D. Comins, L. Cornish, P.A. Olubambi, C.N. Machio, *Corros. Sci*., 51 (2009) 1364.
47. El-Sayed M. Sherif, J.H. Potgieter, J.D. Comins, L. Cornish, P.A. Olubambi, C.N. Machio, *J. Appl. Electrochem*., 39 (2009) 1385.
48. El-Sayed M. Sherif, *Int. J. Electrochem. Sci*., 6 (2011) 2284.
49. El-Sayed M. Sherif, *Int. J. Electrochem. Sci*., 7 (2012) 2374.
50. M. Abdallah, *Mater. Chem. Phys*., 82 (2003) 786.
51. Rongguang Wang, Mitsuo Kido, Mater. Trans., 48 (2007) 1451.